Performance Analysis of Dynamic Lightpath Configuration for WDM Asymmetric Ring Networks

Takuji Tachibana and Shoji Kasahara

Graduate School of Information Science
Nara Institute of Science and Technology
Takayama 8916-5, Ikoma, Nara 630-0101, Japan
{takuji-t, kasahara}@is.aist-nara.ac.jp

Abstract. In this paper, we analyze the performance of a lightpath configuration method for optical add/drop multiplexer (OADM) in WDM asymmetric ring network. We consider a multiple queueing system for a node in the ring network and derive loss probability and wavelength utilization factor. Numerical examples show how arrival rate from access network and the threshold specified in the dynamic configuration method affect loss probability and wavelength utilization factor. In addition, comparing the proposed method with static configuration method, the loss probability under the proposed method can be almost the same as that under the static method where lightpaths are pre-established such that all wavelengths in the network are used efficiently.

1 Introduction

Optical add/drop multiplexer (OADM) selectively adds/drops wavelengths at any OADM to establish lightpaths in WDM network [3,4,6,7,9,11]. This provides all-optical connection between any pair of OADMs (see Fig. 1). The number of available wavelengths is 16, 32, 64, 128 and so on, and the wavelengths to be added/dropped are pre-selected in each OADM [5,8,10]. Hence significant pre-deployment network planning is required to specify what and where wavelengths are to be added/dropped. Once the network design is determined, the design will not be changed unless network operator is willing to change the network design. When the traffic pattern changes frequently, the OADM degrades the performance of network [13]. However, if wavelengths are dynamically allocated, high utilization of wavelengths and large throughput of packets are expected [2].

To realize dynamic lightpath configuration for OADM, we have proposed a dynamic lightpath configuration method [12]. With our proposed method, a lightpath is established according to the congestion state of a node and is released when there are no packets to be transmitted in a buffer for the lightpath. It is not necessary to pre-select added/dropped wavelengths.

In [12], we have considered the WDM ring network as shown in Fig. 2 where traffic is injected into each node from each access network at the same rate. Under

E. Gregori et al. (Eds.): NETWORKING 2002, LNCS 2345, pp. 972–983, 2002.

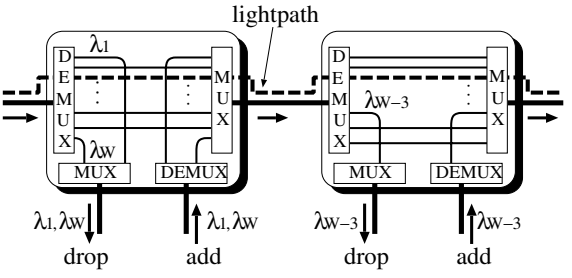

Fig. 1. Optical add/drop multiplexer.

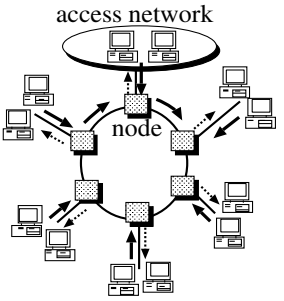

Fig. 2. Ring network model.

the real network environment, however, traffic volume injected from an access network depends on its location and services provisioned, i.e., traffic volume from each access network is different; we call such ring network an WDM asymmetric ring network.

To analyze performances of the dynamic lightpath configuration method for WDM asymmetric ring network, we further extend the symmetric ring network model in [12] to an asymmetric one. We model this system as a continuous-time Markov chain and derive the loss probability of packets coming from access network to node and wavelength utilization factor. With the analysis and simulation, we investigate how arrival rate from access network and the threshold specified in the lightpath configuration method affect the performance measures for WDM asymmetric ring network. Finally, we compare the proposed method with static configuration method and discuss the effectiveness of the proposed method.

The rest of the paper is organized as follows. Section 2 summarizes the dynamic lightpath configuration method, and in Section 3, we present the analytical model of our proposed method for WDM asymmetric ring networks. The performance analysis in the case of light traffic is presented in Section 4 and numerical examples are given in Section 5. Finally, conclusions are presented in Section 6.

2 Dynamic Lightpath Configuration Method

In this section, we summarize the dynamic lightpath configuration method proposed in [12]. Each node consists of an OADM with MPLS control plane and a label switching router (LSR) [1,2]. The procedure of lightpath configuration is as follows (see Fig. 3).

For simplicity, we consider a tandem network with three nodes, namely, nodes A, B and C. Each node is connected to its own access network through LSR. Suppose $W+1$ wavelengths are multiplexed into an optical fiber in our network. Among $W+1$ wavelengths, W wavelengths are used to transmit data traffic and one is dedicated to carry and distribute control traffic. Therefore we handle W wavelengths that consist of one default path and $W-1$ lightpaths.

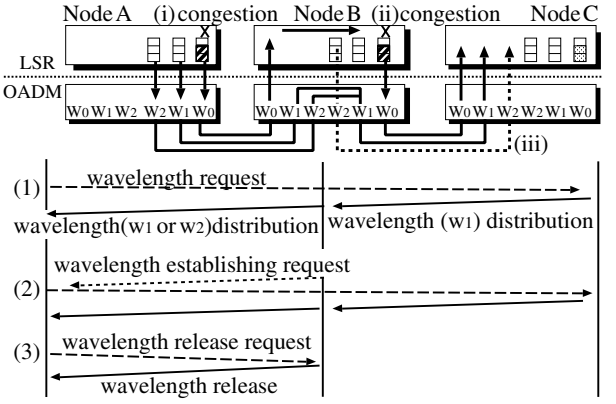

Fig. 3. Dynamic lightpath configuration.

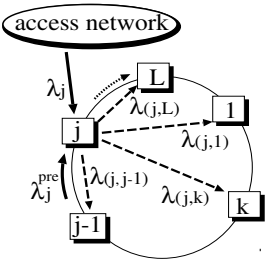

Fig. 4. Traffic from node j to other nodes.

Let w_0 denote a wavelength for default path used between adjacent nodes (A and B or B and C in Fig. 3). We define w_i $(1 \leq i \leq W-1)$ as the wavelength which is dynamically allocated according to congestion in default path.

If an IP packet whose destination is node C arrives at node A from access network, the LSR in node A performs label switching by establishing a relation between <input port, input label> tuple and <output port, output label> tuple according to its destination node. Through MPLS control plane, OADM determines a relevant output wavelength corresponding to the output label. If the default path is not congested and a lightpath is not established between nodes A and C, the packet is transmitted to node B with wavelength w_0. When the packet arrives at node B, the LSR in node B performs label switching. Then, through MPLS control plane, the OADM in node B determines output wavelength and the packet is transmitted to node C with it.

An LSR in each node has W buffers corresponding to W wavelengths. In particular, the buffer for default path (default buffer) has pre-specified threshold. If the number of packets in default buffer becomes equal to or greater than the threshold, LSR regards the default path as being in congestion and decides to establish a new lightpath. Here the new lightpath is established between the source and destination nodes of the packet that triggers the congestion. The new lightpath is established in the following manner. Now we consider the two cases: the packet that is transmitted from nodes A to C (i) triggers congestion at node A and (ii) triggers congestion at node B.

In the case of (i), the MPLS control plane in node A requests a wavelength to the MPLS control plane in node C for the establishment of a new lightpath using control traffic (Fig. 3 (1)). Distributing network state information, MPLS control plane in each node has the latest information of lightpath configuration all the time. When the wavelength request of node A arrives at node C, MPLS control plane in node C searches an available wavelength for path BC. If wavelength

w_1 is available for path BC, node C informs node B that w_1 is available using control signal and adjusts its OADM to drop w_1.

Subsequently, the MPLS control plane in node B searches an available wavelength for path AB. If w_1 is also available for path AB, node B informs node A about it. Otherwise, node B informs node A of another wavelength, say w_2. In the latter case, w_2 is converted to w_1 at node B for the transmission from A to C. If no wavelengths are available, the new lightpath establishment fails.

Finally, node A adjusts its OADM to add w_1 or w_2. Until the lightpath establishment is completed, wavelength w_0 is still used for the packet transmission between A and C. As soon as the establishment is completed, the lightpath becomes available.

In the case of (ii) where congestion occurs at intermediate node B, the MPLS control plane in node B asks node A to request a new wavelength to node C (Fig. 3 (2)). Successive procedure is same as the case (i).

If there are no packets in the buffer after packet transmission, the timer for the holding time starts. The established lightpath is released if the holding time is over and there are no packets in the buffer (Fig. 3 (iii), (3)).

For simplicity, we assume in the paper that multiple lightpaths between any pair of nodes are not permitted.

3 System Model

We consider a WDM network where L nodes are connected in ring topology (see Fig. 2). Each node, as shown in the previous section, consists of OADM with MPLS control plane and LSR and establishes/releases lightpaths according to the dynamic lightpath configuration method. In addition, each node is connected to its own access network through LSR.

We assume that the number of wavelengths available at each node is W and all wavelengths can be converted regardless of any wavelength pairs. One of W wavelengths is for a default path and the others are for lightpaths which are dynamically established. $W-1$ wavelengths for lightpaths are numbered from 1 to $W-1$. A lightpath is established with a wavelength which has the smallest number. When there are no idle wavelength up to the $i-1$th one, a lightpath is established with the ith $(1 \leq i \leq W-1)$ wavelength.

We have two types of buffers in each node: one is for default path and the others are for lightpaths which are dynamically established/released. Let K_d denote the capacity for default buffer and K_l the capacity for each lightpath buffer. Here, the buffer capacity consists of a waiting room where packets wait for transmission and a server where a packet is in transmission. Let T_h denote the pre-specified value of threshold for default path.

For traffic condition within this WDM asymmetric ring network, we assume that packets arriving at node j $(1 \leq j \leq L)$ from access network are transmitted to destination nodes in clockwise direction. Under this assumption, we have two kinds of packet traffic that arrives at the node j: one is from the access network and the other is from the previous node $j-1$ as shown in Fig. 4.

In terms of traffic from the access network, we assume that packets arrive at node j from access network according to a Poisson process with parameter λ_j. We assume that for $1 \leq j \leq L$, λ_j is so small that packet loss hardly occurs at intermediate nodes. Moreover we assume that the destination of a packet which arrives at node j is k ($k \neq j$) with probability $P_k^{(j)}$ which satisfies $\sum_{\substack{k=1 \\ k \neq j}}^{L} P_k^{(j)} = 1$.

Therefore, packets sent to the destination k arrive at node j from access network according to a Poisson process with parameter $\lambda_{(j,k)}$ which is given by

$$\lambda_{(j,k)} = P_k^{(j)} \lambda_j. \tag{1}$$

Next we consider traffic which arrives at node j from node $j-1$. Since the buffers in each node are finite queues, our ring network is not an open Jackson queueing network. Due to light traffic, however, arrival packets are hardly lost and most of packets are served by default path. Therefore we can approximate the arrival process from previous node with the similar approach to the analysis of open Jackson network [14].

Let λ_j^{pre} denote the arrival rate of the packet arrival process from node $j-1$ to node j. Noting that packets are sent in clockwise direction and hardly lost due to light traffic assumption, λ_j^{pre} can be approximated with the following:

$$\lambda_j^{pre} \simeq \sum_{k=1}^{j-1} \left\{ \sum_{n=j+1}^{L} \lambda_{(k,n)} + \sum_{m=1}^{k-1} \lambda_{(k,m)} \right\} + \sum_{k=j+2}^{L} \sum_{n=j+1}^{k-1} \lambda_{(k,n)}, \quad 1 \leq j \leq L. \tag{2}$$

We assume that the packet arrival process at node j from the previous node $j-1$ is Poisson with rate λ_j^{pre}.

The whole packets arrive at the node j according to a Poisson process with rate $\lambda_j^{all} = \lambda_j + \lambda_j^{pre}$ which is given by

$$\lambda_j^{all} = \sum_{k=1}^{j} \left\{ \sum_{n=j+1}^{L} \lambda_{(k,n)} + \sum_{m=1}^{k-1} \lambda_{(k,m)} \right\} + \sum_{k=j+2}^{L} \sum_{n=j+1}^{k-1} \lambda_{(k,n)}, \quad 1 \leq j \leq L. \tag{3}$$

We define $D_l^{(j)}(t)$ as the set of destination nodes of the established lightpaths in node j at t. Then packets arrive at default path according to a Poisson process with rate $\lambda_j^{all} - \lambda_j^{light}$ where λ_j^{light} is given by

$$\lambda_j^{light} = \sum_{k \in D_l^{(j)}(t)} \lambda_{(j,k)}. \tag{4}$$

We also assume that for any node the transmission time of a packet, the lightpath establishment/release time and the holding time are exponentially distributed with rates μ, p and h, respectively.

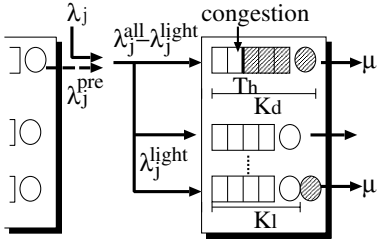

Fig. 5. Asymmetric ring node model with light traffic.

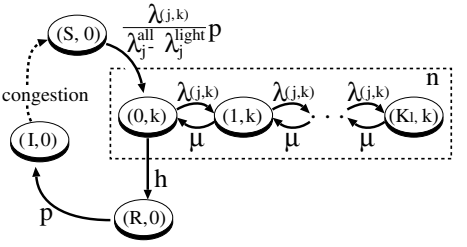

Fig. 6. State transition diagram for a lightpath $l_i^{(j)}$.

4 Performance Analysis

We consider a multiple queueing system for node j $(1 \leq j \leq L)$ illustrated in Fig. 5.

Let $l_i^{(j)}$ $(1 \leq i \leq W)$ denote the ith lightpath dynamically established/released at node j. We define the state of a lightpath $l_i^{(j)}$ $(1 \leq i \leq W-1)$ for node j at t as

$$J_{l_i}^{(j)}(t) = \begin{cases} n, (0 \leq n \leq K_l), & \text{if } l_i^{(j)} \text{ is busy,} \\ I, & \text{if } l_i^{(j)} \text{ is idle,} \\ S, & \text{if } l_i^{(j)} \text{ is being established,} \\ R, & \text{if } l_i^{(j)} \text{ is being released.} \end{cases}$$

Let $N_d^{(j)}(t)$ denote the number of packets in default path for node j at t. $d_{l_i}^{(j)}(t)$ is defined as the destination node directly connected with lightpath $l_i^{(j)}$ at t and given by

$$d_{l_i}^{(j)}(t) = \begin{cases} k, & \text{if } l_i^{(j)} \text{ is busy and connected to node } k\ (\in D_l^{(j)}(t)), \\ 0, & \text{otherwise.} \end{cases} \tag{5}$$

Finally, we define the state of the system at t as

$$(N_d^{(j)}(t),\ \boldsymbol{J}_l^{(j)}(t)), \tag{6}$$

where $\boldsymbol{J}_l^{(j)}(t)$ is given by

$$\boldsymbol{J}_l^{(j)}(t) = (\,(J_{l_1}^{(j)}(t),\ d_{l_1}^{(j)}(t)), \cdots, (J_{l_{W-1}}^{(j)}(t),\ d_{l_{W-1}}^{(j)}(t))\,). \tag{7}$$

In addition, we define $M_{l^{(j)}}^I(t)$ as the number of idle lightpaths at t, and it is expressed as

$$M_{l^{(j)}}^I(t) = \sum_{i=1}^{W-1} 1_{\{J_{l_i}^{(j)}(t)=I\}}, \tag{8}$$

where $1_{\{X\}}$ is the indicator function of event X.

Table 1. State transition rate in asymmetric ring network model.

Number of active lightpaths	Current state $(N_d,\ \boldsymbol{J}_l)$	Next state	Transition rate
$M_l^I > 0$	$N_d < T_h$	$(N_d+1,\ \boldsymbol{J}_l)$	$\lambda_j^{all} - \lambda_j^{light}$
	$T_h \le N_d < K_d$, $(J_{l_{i_I^{\min}}}, d_{l_{i_I^{\min}}}) = (I,\ 0)$	$(N_d+1,\ \boldsymbol{J}_l)$, $(J_{l_{i_I^{\min}}}, d_{l_{i_I^{\min}}}) = (S,\ 0)$	$\lambda_j^{all} - \lambda_j^{light}$
	$N_d = K_d$, $(J_{l_{i_I^{\min}}}, d_{l_{i_I^{\min}}}) = (I,\ 0)$	$(N_d,\ \boldsymbol{J}_l)$, $(J_{l_{i_I^{\min}}}, d_{l_{i_I^{\min}}}) = (S,\ 0)$	$\lambda_j^{all} - \lambda_j^{light}$
	$N_d > 0$	$(N_d-1,\ \boldsymbol{J}_l)$	μ
$M_l^I = 0$	$N_d < K_d$	$(N_d+1,\ \boldsymbol{J}_l)$	$\lambda_j^{all} - \lambda_j^{light}$
	$N_d > 0$	$(N_d-1,\ \boldsymbol{J}_l)$	μ

State of lightpaths	Current state $(N_d,\ \boldsymbol{J}_l)$	Next state $(N_d,\ \boldsymbol{J}_l)$	Transition rate
$(J_{l_i}, d_{l_i}) = (S,\ 0)$	-	$(J_{l_i}, d_{l_i}) = (0,\ k)$	$\frac{\lambda_{(j,\,k)}}{\lambda_j^{all} - \lambda_j^{light}} p$
$(J_{l_i}, d_{l_i}) = (n,\ k)$	$n < K_l$	$(J_{l_i}, d_{l_i}) = (n+1,\ k)$	$\lambda_{(j,\,k)}$
	$n > 0$	$(J_{l_i}, d_{l_i}) = (n-1,\ k)$	μ
	$n = 0$	$(J_{l_i}, d_{l_i}) = (R,\ 0)$	h
$(J_{l_i}, d_{l_i}) = (R,\ 0)$	-	$(J_{l_i}, d_{l_i}) = (I,\ 0)$	p

The state transition diagram for $l_i^{(j)}$ is illustrated in Fig. 6. Let $U^{(j)}$ denote the whole state space of $(N_d^{(j)}(t),\ \boldsymbol{J}_l^{(j)}(t))$ and $U_l^{(j)}$ the space comprised of $\boldsymbol{J}_l^{(j)}(t)$.

In the remainder of this subsection, the argument t is omitted since we consider the system in equilibrium.

The transition rate from the state $(N_d^{(j)},\ \boldsymbol{J}_l^{(j)})$ is shown in Table 1. Note that we omit the superscript (j) of any notation for the simplicity. $i_I^{\min}$ in Table 1 is defined as

$$i_I^{\min} = \min\{\, i\,;\, J_{l_i}^{(j)} = I,\ 1 \le i \le W-1\}. \tag{9}$$

For example, when current state is $(N_d^{(j)},\ \boldsymbol{J}_l^{(j)})$ where $M_{l^{(j)}}^I > 0, T_h \le N_d^{(j)} < K_d$ and the state of $l_i^{(j)}$ is idle, a packet arrives at default path with rate $\lambda_j^{all} - \lambda_j^{light}$. Then N_d is increased by one and the lightpath establishment of $l_i^{(j)}$ starts. Similarly, when current state is $(N_d^{(j)},\ \boldsymbol{J}_l^{(j)})$ where an established lightpath $l_i^{(j)}$ has no packets in its own buffers, the holding time of $l_i^{(j)}$ is over with rate h and $l_i^{(j)}$ is released.

Let $\pi(N_d^{(j)},\ \boldsymbol{J}_l^{(j)})$ represent the steady state probability of $(N_d^{(j)},\ \boldsymbol{J}_l^{(j)})$. $\pi(N_d^{(j)},\ \boldsymbol{J}_l^{(j)})$ is uniquely determined by equilibrium state equations and following normalized condition

$$\sum_{(N_d^{(j)}, \boldsymbol{J}_l^{(j)}) \in U^{(j)}} \pi(N_d^{(j)},\ \boldsymbol{J}_l^{(j)}) = 1. \tag{10}$$

Equilibrium state equations are omitted due to page limitation.

With $\pi(N_d^{(j)},\ \boldsymbol{J}_l^{(j)})$, loss probability $P_{loss}^{(j)}$ and wavelength utilization factor $P_{wave}^{(j)}$ for node j are given by

$$P_{loss}^{(j)} = \sum_{(K_d^{(j)},\boldsymbol{J}_l^{(j)})\in U^{(j)}} \left\{1 - \frac{\lambda_j^{light}}{\lambda_j^{all}}\right\} \pi(K_d^{(j)},\ \boldsymbol{J}_l^{(j)}) + \sum_{N_d^{(j)}=0}^{K_d} \sum_{i=1}^{W-1} \sum_{d_{l_i}^{(j)}\in D_l^{(j)}} \sum_{\substack{\boldsymbol{J}_l^{(j)}\in U_l^{(j)} \\ J_{l_i}^{(j)}=K_l}} \pi(N_d^{(j)},\ \boldsymbol{J}_l^{(j)}) \frac{\lambda_{(j,k)}}{\lambda_j^{all}}, \tag{11}$$

$$P_{wave}^{(j)} = \sum_{(N_d^{(j)},\boldsymbol{J}_l^{(j)})\in U^{(j)}} \left\{1_{\{N_d^{(j)}>0\}} + \sum_{i=1}^{W-1} 1_{\{(J_{l_i}^{(j)},\, d_{l_i}^{(j)})\neq(I,0)\}}\right\} \frac{\pi(N_d^{(j)},\ \boldsymbol{J}_l^{(j)})}{W}. \tag{12}$$

5 Numerical Examples

In our numerical examples, we assume that a labeled packet size (an IP datagram + a label) is 1250 bytes within access networks and that the transmitting speed of each wavelength is 10 Gbps. Thus, the transmission speed is calculated as

$$\frac{1250\ [\text{byte}] \times 8\ [\text{bit/byte}]}{10\ [\text{Gbps}]} = 1\ [\mu\text{s}]\,. \tag{13}$$

We set $1/\mu = 1$ [μs], where $1/\mu$ is the mean transmission time of a packet.

We set both the lightpath establishment/release time and holding time are equal to 1.0 [ms], i.e., $p = 0.001$ and $h = 0.001$. In this section, we consider WDM asymmetric ring network where there are 10 nodes.

5.1 Impact of Traffic Volume from Access Network

Figs. 7 and 8 illustrate how traffic volume from access network affects loss probability. In both figures, we set $W = 4$, $K_d = 6$, $K_l = 5$ and $T_h = 4$, and assume that the destination of each packet is equally likely, i.e., for any pair nodes j and k ($k \neq j$),

$$P_k^{(j)} = \frac{1}{L-1} = \frac{1}{9}. \tag{14}$$

Moreover arrival rate at node 1 from access network, λ_1, is variable and other arrival rates are fixed and equal to 0.015.

Fig. 7 shows the numerical result calculated by approximation analysis and Fig. 8 represents simulation result. We observe the quantitative discrepancy between Figs. 7 and 8. This is because the loss probability in Fig. 7 is calculated under the assumption of exponential distributions of transmission time, lightpath establishment/release time and holding time while those times are set to be

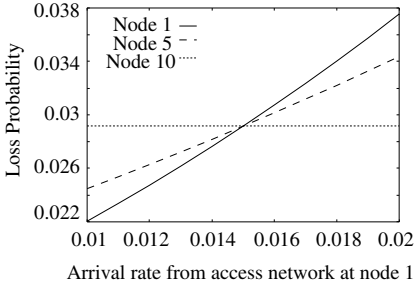

Fig. 7. Loss probability vs. arrival rate: approximation analysis.

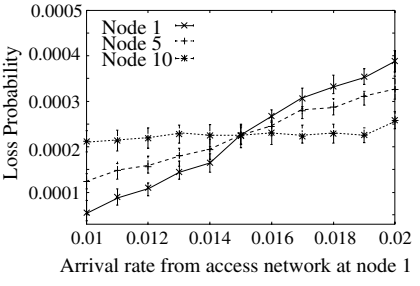

Fig. 8. Loss probability vs. arrival rate: simulation.

constant in simulation. However, both figures show the same tendency and hence our analytical model is useful for capturing the loss behavior under proposed method in a qualitative sense.

Our numerical experiments also show that our analytical model succeeds in capturing the characteristic of wavelength utilization factor, however, we omit those results due to page limitation.

In Figs. 7 and 8, we observe that loss probability for node 1 increases as arrival rate at node 1 increases while loss probability for node 10 is constant. Since destinations of packet streams originated in node 1 are equally likely, the arrival rate from previous node $j-1$, λ_j^{pre}, becomes small as the node-number j increases. This results in the small (large) loss probability if λ_1 is smaller (larger) than λ_j ($j = 2, \cdots, 10$). We further investigate this tendency in the next subsection.

5.2 Impact of Node Position

In this subsection, with our analytical result, we investigate how the loss probability and wavelength utilization factor of each node differ from those of other nodes.

Here, we set $W = 4$, $K_d = 30$, $K_l = 5$ and $T_h = 20$. The destination of each packet is equally likely, i.e., $P_k^{(j)} = 1/9$.

In terms of traffic volume from each access network, we consider the following types;

$$\text{Type A: } \lambda_i = \begin{cases} 0.18, & i = 1, 6, \\ 0.135, & \text{otherwise.} \end{cases} \qquad \text{Type B: } \lambda_i = \begin{cases} 0.09, & i = 1, 6, \\ 0.135, & \text{otherwise.} \end{cases}$$

Fig. 9 shows the loss probability against the position of node. From Fig. 9, we observe that loss probability depends on the distance from node 1 or node 6. For type A, nodes 1 and 6 have larger loss probability than others while for type B, nodes 5 and 10 have larger loss probability than others. For type A, λ_1 and λ_6 are larger than others and this makes LSRs of nodes 1 and 6 in congestion.

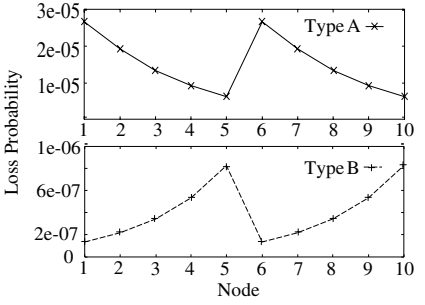

Fig. 9. Loss probability vs. node position.

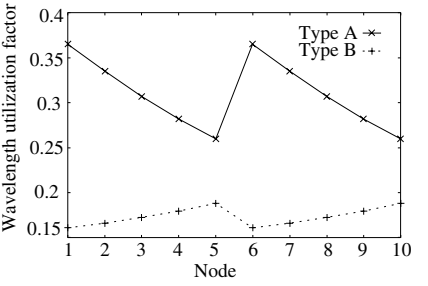

Fig. 10. Wavelength utilization factor vs. node position.

This causes the large loss probabilities of nodes 1 and 6. On the other hand, the packet streams originated in node 1 leave the ring network at nodes 2, 3, $\cdots$, and 10 in this order and hence the total arrival rate becomes small as the node-number increases. This results in the decrease of loss probabilities from nodes 2 to 5. At node 6, the same traffic volume is injected and this causes the jump of loss probability. The decrease of loss probability from nodes 6 to 10 follows from the same reason.

For type B, λ_1 and λ_6 are smaller than others and this causes the small loss probabilities at nodes 1 and 6. As the node-number increases, the traffic volume larger than λ_1 and λ_6 makes the network being congested and this results in the increase of loss probabilities at nodes from 2 (7) to 5 (10).

Fig. 10 illustrates how the proposed method establishes lightpaths in the asymmetric network. From this figure, we find that the proposed method can establish lightpaths according to traffic volume originated in each node. For type A, nodes 1 and 5 establish more lightpaths than others and for type B, nodes 6 and 10 establish more lightpaths than others. From this figure, we observe that the dynamic lightpath establishment function works well for WDM asymmetric ring network.

5.3 Impact of Threshold

In this subsection, we investigate how the threshold affects loss probability with our analytical result. We set $W = 4$, $K_d = 30$ and $K_l = 5$. As is the case with the above sections, we assume that the destination of each packet is equally likely, and consider the traffic condition for type A.

Fig. 11 shows how loss probability is affected by threshold. From Fig. 11, we observe that smaller threshold gives smaller loss probability. This is because the LSR with small threshold regards the node as being in congestion frequently and makes lightpaths busy. We also find that loss probabilities for nodes 5 and 10 do not change so much while those for nodes 1 and 6 decrease as threshold

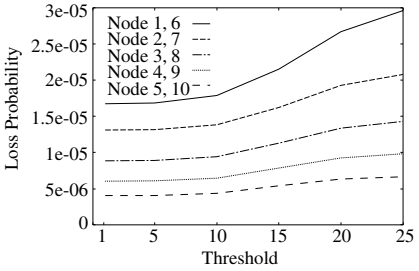

Fig. 11. Loss probability vs. threshold.

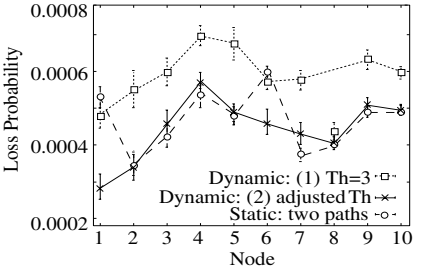

Fig. 12. Comparison of dynamic and static configurations: simulation.

becomes small. Therefore small threshold is effective to improve loss probabilities of bottleneck nodes.

5.4 Comparison of Dynamic and Static Configurations

Finally, we compare the proposed method with static configuration method where wavelengths are allocated to lightpaths statically.

Fig. 12 illustrates loss probability for each node in cases of the proposed method and static configuration method. Loss probabilities in Fig. 12 are calculated by simulation. In this figure we set $W = 4$, $K_d = 6$, $K_l = 5$ and consider the traffic condition for type A. In addition, $P_k^{(j)}$=1/9 for all j and k ($j \neq k$) except $j = 1$ and 6. For $j = 1$ and 6, we set

$$P_k^{(1)} = \begin{cases} 0.08, & k = 2, 3, \\ 0.12, & \text{otherwise.} \end{cases} \qquad P_k^{(6)} = \begin{cases} 0.08, & k = 7, 8, \\ 0.12, & \text{otherwise.} \end{cases}$$

That is, more packets whose destinations are nodes 2 (7) or 3 (8) arrive at node 1 (6) than packets whose destinations are other nodes.

As for the static configuration method, we consider the case where each node statically establishes two lightpaths: one is connected to the next node and the other is connected to the next but one. Note that this is the most efficient use of wavelengths for the ring network considered here.

As for the dynamic configuration, we consider the following two cases: (1) $T_h = 3$ for all nodes and (2) T_h's are different such as

$$T_h = \begin{cases} 1, \ k = 1, 6, & 3, \ k = 3, 4, 8, 9, \\ 2, \ k = 2, 7, & 4, \ k = 5, 10. \end{cases}$$

The case of (2) is based on the results of the previous subsections.

From Fig. 12, we observe that the loss probability for dynamic configuration with $T_h = 3$ is the largest and that the loss probability for the proposed method with adjusted T_h's is almost equal to or lower than that for static configuration case. This suggests that the proposed method can establish lightpaths efficiently between pairs of nodes whose traffic volume is large.

6 Conclusion

In this paper, we have analyzed the performance of the dynamic wavelength allocation method for WDM asymmetric ring network. Numerical examples have showed that the proposed method can establish lightpaths efficiently according to traffic volume from access network even when some nodes are in congestion. In addition, the loss probability under the proposed method can be almost the same as that under the static method where lightpaths are pre-established such that all wavelengths in the network are used efficiently.

References

1. D. O. Awduche, "MPLS and Traffic Engineering in IP Networks," *IEEE Communications Magazine*, vol. 37, no. 12, pp. 42-47, Dec. 1999.
2. D. O. Awduche et al., "Multi-Protocol Lambda Switching: Combining MPLS Traffic Engineering Control With Optical Crossconnects," IETF draft-awduche-mpls-te-optical-03.txt, Apr. 2001.
3. P. Bonenfant, and A. R. Moral, "Optical Data Networking," *IEEE Communications Magazine*, vol. 38, no. 3, pp. 63-70, Mar. 2000.
4. I. Chlamtac, V. Elek, A. Fumagalli, and C. Szabó, "Scalable WDM Access Network Architecture Based on Photonic Slot Routing," *IEEE/ACM Trans. Networking*, vol. 7, no. 1, pp. 1-9, Feb. 1999.
5. O. Gerstel, R. Ramaswami, and G. H. Sasaki, "Cost-Effective Traffic Grooming in WDM Rings," *IEEE/ACM Trans. Networking*, vol. 8, no. 5, pp. 618-630, Oct. 2000.
6. N. Ghani, S. Dixit, and T. S. Wang, "On IP-over-WDM Integration," *IEEE Communications Magazine*, vol. 38, no. 3, pp. 72-84, Mar. 2000.
7. M. W. McKinnon, H. G. Perros, and G. N. Rouskas, "Performance Analysis of Boadcast WDM Networks under IP Traffic," *Performance Evaluation*, vols. 36-37, pp. 333-358, Aug. 1999.
8. Y. Miyao, "λ-Ring System: An Application in Survivable WDM Networks of Interconnected Self-Healing Ring Systems," *IEICE Trans. Commun.*, vol. E84-B, no. 6, June, 2001.
9. B. Ramamurthy, and B. Mukherjee, "Wavelength Conversion in WDM Networking," *IEEE J. Select. Areas Commun.*, vol. 16, no. 7, pp. 1061-1073, Sep. 1998.
10. R. Ramaswami, and K. N. Sivarajan, *Optical Networks: A Practical Perspective*. San Francisco: Morgan Kaufmann Publishers, 1998.
11. K. Sato, S. Okamoto, and H. Hadama, "Network Performance and Integrity Enhancement with Optical Path Layer Technologies," *IEEE J. Select. Areas Commun.*, vol. 12, no. 1, pp. 159-170, Jan. 1994.
12. T. Tachibana and S. Kasahara, "Performance Analysis of Dynamic Lightpath Configuration with GMPLS for WDM Ring Networks: The Light Traffic Case," Technical Report of IEICE (NS2001-140), pp.37-42, 2001.10.19. (in Japanese) .
13. W. Weiershausen, A. Mattheus, and F. Küppers, "Realisation of Next Generation Dynamic WDM Networks by Advanced OADM Design," *WDM and Photonic Networks*, D. W. Faulkner, and A. L. Harmer eds., IOS Press, Amsterdam, pp. 199-207, 2000.
14. R. W. Wolff, *Stochastic Modeling and the Theory of Queues*. New Jersey: Prentice Hall, 1989.